

Experimental Demonstration of a Single Acoustic Vector Sensor for JANUS Performance Enhancement

Fabrizio A. Bozzi and Sérgio M. Jesus

Laboratory for Robotic Systems in Engineering and Science (LARSyS)

University of Algarve

8005-139 Faro, Portugal

fabozzi@ualg.pt, sjesus@ualg.pt

Abstract—This study shows the underwater communication performance using an acoustic pressure-gradient vector sensor. Combining the estimated particle velocity channels with the acoustic pressure results in a cardioid-like beam steered output, which is used to improve the signal-to-noise ratio. A shallow-water field experiment was carried out using a single vector sensor as a receiver and a ship-suspended sound source, transmitting the frequency-hopped JANUS modulated signal at several ranges and directions. Bit error rate analysis demonstrates how performance can be enhanced through vector sensor channel combining. Firstly, by relating the error with beam pattern varying the azimuth steering angle. Second, by relating the error with transmitting stations, where individual channels of the vector sensor can be compared. Besides such findings, this study also presents tools for better understanding the directional characteristic, such as the design factor to combine the particle velocity to the pressure sensor and azigrams. Finally, results show that the JANUS bit error rate can be reduced up to five percent by combining the vector sensor components compared to the pressure sensor.

Index Terms—acoustic vector sensor, particle velocity, underwater acoustic communications, JANUS

I. INTRODUCTION

Acoustic vector sensors' compactness is an attractive characteristic for size-restricted underwater applications. The directional capability of vector sensors comes from the particle velocity (or its derivatives), which may be estimated by pressure-gradient or inertial sensors [1]. Vector sensors have been used since the 80s in the directional sonobuoys for sonar applications [2]. Its usage was mainly focused on lower frequency bands (< 1 kHz), where some bearing discrimination could be achieved by a single collocated device. For communications, vector sensors are relatively new, and available work is dated from 2007 [3]. In the reduced literature on vector sensors for communications, scarcely anything regards the technological design for particle velocity estimation and its impact on performance. Thus, this is the first aspect that the present study addresses, pre-processing the particle velocity and pressure-difference channels. Then, a channel combining approach is employed, where the vector sensor channels are weighted and combined in a beam steering approach [4]. This channel combining approach is already

used for sonar applications, and here, its impact on the bit error rate performance is analyzed. One can notice that this study does not intend to compare either the several direction-of-arrival techniques available (e.g., [5]–[9]) or communication techniques, such as passive time-reversal [10], which have already been discussed in the vector sensors field. Moreover, the major literature concerning direction-of-arrival estimation has shown that many of the high spatial resolution techniques do not imply the signal-to-noise increment and thus are not guaranteed to be advantageous for communications. Furthermore, some techniques are computationally expensive and unsuitable if we think of a practical low-power system. Thus, the motivation for using such a beam steering approach consists on: its simplicity, which is a practical and low-power demanding, suited for hardware of opportunity; and its robustness for variable ambient noise levels [7].

This study uses the frequency-hopped JANUS modulation, a well-known robust communication option [11]–[14]. Advantages of JANUS are: standardization, interoperability, and its easy employment with open-source codes. In this study, the use of a vector sensor for JANUS has as objective to allow faster bit rate, by improving SNR [14], but one can think in a multiple sources scenario usage, where the azimuth spatial filter may also be useful. Here, the communication performance is quantified using data from a shallow-water experiment, where a two-axis vector sensor was placed near the bottom and transmissions were performed using a sound source tied to a ship. The BER is quantified before the JANUS interleaved stage and the relation between the bit error and the beam response is shown. Two center frequencies are analyzed and the comparison with the pressure-only sensor shows the performance enhancement.

II. THEORETICAL FRAMEWORK

A. Data model

A single acoustic vector sensor has the n -th output:

$$r_n = h_n \otimes s + w_n, \quad (1)$$

where h is the channel impulse response, s is the transmitted signal, and w is the additive noise. The index n refers,

from 1 to 3, to the pressure, x and y horizontal particle velocity components, respectively. The \otimes symbol stands for time convolution. Whereas (1) is commonly used to represent single-input multiple-output (SIMO) communication systems with pressure sensors, the particle velocity components are directional channels. A particle velocity component may be seen through the Euler's equation:

$$v = -\frac{1}{j\omega\rho_0} \nabla p, \quad (2)$$

where v is the particle velocity, ∇ is the gradient operator, p is the pressure, ω is the angular frequency, and ρ_0 is the medium static density. Assuming plane-wave condition, $p_v = -\rho_0 c v$, where c is the sound speed and p_v is the so-called pressure-equivalent particle velocity. Thus, (2) becomes:

$$p_v = \frac{1}{jk} \nabla p, \quad (3)$$

where $k = \omega/c = 2\pi/\lambda$ is the wavenumber, being λ the wavelength. The pressure difference between two identical, closed spaced (s), omnidirectional pressure sensors is given as [4]:

$$\Delta p = j2p_0 \sin\left(\frac{k's' \cos\theta}{2}\right) \approx jp_0 k's' \cos\theta, \quad \because \lambda \ll s \quad (4)$$

where p_0 is a pressure reference, θ is the angle between the propagation direction and the pressure sensors axis, and the superscript $[]'$ is used to represent an unknown parameter. Considering the first-order approximation $\frac{\Delta p}{s} = \frac{\partial p}{\partial s}$ and replacing (4) in (3) gives:

$$p_v = \frac{1}{jk} \frac{\Delta p}{s} = \frac{1}{jks} jp_0 k's' \cos\theta, \quad (5)$$

where if $k' = k$, $s' = s$, and the plane-wave assumption is valid for the operational frequency range, then (5) becomes:

$$p_v = p_0 \cos\theta. \quad (6)$$

One can note some aspects of the developed equations: (4) is the output of a pressure-gradient vector sensor, which is frequency-spacing dependent, a drawback characteristic; (6) is not frequency-dependent, but in practice, technological issues make it difficult to guarantee those matched conditions, e.g., identical sensors and that $\lambda \ll s$; and the noise characteristic may be affected by the difference operation, which may lead to non-isotropic noise, not treated in this study. Except for these aspects, there are two possible ways to process the vector sensor directional channels, either by using the pressure-difference output (Δp) or by estimating the particle velocity (p_v). The latter is performed using the middle term of (5), where s and c are approximated values.

B. Vector sensor receiver structure

The receiver structure is a multichannel system where the n -th input is the r_n vector sensor channel. The vector sensor channel combining output (y_{bs} , called hereafter vector sensor beam steering) is given by:

$$y_{bs} = r_p + \delta[r_{vx} \cos\theta_0 + r_{vy} \sin\theta_0], \quad (7)$$

where, r_p , r_{vx} , and r_{vy} are the pressure and pressure-equivalent particle velocity channels. δ is a design factor adjusted according to a desired beam response, and θ_0 is a chosen steering angle, where DoA estimation methods can be used. There are several DoA estimators available in literature but here, the Bartlett estimator is used, where the beam response in the f single frequency is given as:

$$\mathbf{B}(f, \delta, \theta) = [1 \cos\theta \sin\theta]^H \mathbf{C}(f, \delta) [1 \cos\theta \sin\theta], \quad (8)$$

where $\mathbf{C}(f, \delta) = \frac{1}{N} \sum_{f-\Delta f/2}^{f+\Delta f/2} [R_p \delta R_{vx} \delta R_{vy}]^H [R_p \delta R_{vx} \delta R_{vy}]$ is the sample cross-correlation matrix estimated in the frequency domain, in the Δf bandwidth with N samples, where $R_n \equiv R_n(f)$. The estimated azimuth source direction angle is given by:

$$\hat{\theta}_0(f, \delta) = \arg \max_{\theta} \mathbf{B}(f, \delta, \theta). \quad (9)$$

Thus, we can analyze the BER performance using (7) either varying the $-\pi \leq \theta_0 \leq \pi$ or using the estimated source direction azimuth angle from (9). Interested readers may find complete studies in [15], [16], which consider a three-axis vector sensor where elevation is also used. Note that (7) is a single output that is used as input for JANUS.

III. FIELD EXPERIMENT

A shallow-water underwater communication field experiment took place off the South coast of Portugal on November 24, 2021. The EMSO'21 experiment, as part of the EMSO-PT project, has the objective to test a point-to-point communication link between a surface platform and a bottom receiver. In this experiment, a single vector sensor, attached to a tripod, is fixed close to the bottom receiving communication signals from a sound source tied to a ship. The transmitted signals are JANUS modulated in two center frequencies (f_c) of 5 and 10 kHz, and include the cargo sentence "acoustic vector sensors". Differently from the JANUS description manual [13], which states about using a bandwidth of $W \approx 1/3f_c$, here, the bandwidth is fixed in 2 kHz. Such configuration was proposed to explore bands with approximately constant amplitude, based on the Lubell-916C sound source transmission response.

Figure 1 (a) shows the bathymetry area with: the ship track, the vector sensor tripod position (37.04235°N, -8.16359°W); and the transmitting stations, numbered from 1 to 6, with the range from each station to the vector sensor. In this figure, the axes were set according to vector sensor reference, where the x-component points toward North. The tripod is shown in Fig. 1 (b) with the vector sensor assembled at the top. The used pressure-gradient vector sensor is the Geospectrum M35 [17]. The M35 directional outputs are compass-compensated, where the x-component is compensated to the North and the y-component to the East. A 20 cm wide \times 6 cm of diameter cylinder-type autonomous recorder is attached to one tripod's legs. It synchronously records the three vector sensor channels with a 24-bit resolution and sampling frequency of 39062 Hz. Fig. 1 (c) shows the lateral view, where the sound source was tied at the stern of the ship, at approximately 7 m depth. The

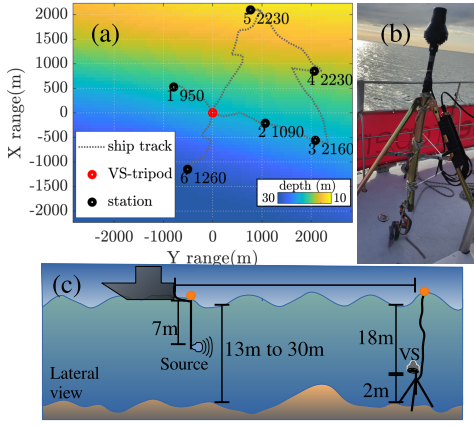


Fig. 1. Bathymetry with the ship track, the vector sensor tripod position, and transmitting stations (a); vector sensor tripod assembling (b); and the experiment geometry lateral view (c).

vector sensor is fixed approximately 2 m from the bottom, where the local water depth is 20 m. The sound speed profile measured during the experiment has a slight variation of around 1516 m/s, and this value is used for the particle velocity estimation. Moreover, the spacing between pressure sensors for the particle velocity estimation is considered $s = 0.05$ m.

IV. RESULTS AND DISCUSSIONS

A. Vector sensor pre-processing analysis

It is crucial to analyze the vector sensor channels in order to understand the particularities of the directional components. The employed vector sensor has an internal compass compensation, which facilitates the first check of the directional components (Δp or p_v) by analyzing their phase, referenced to the omnidirectional sensor. An example can be seen in Fig. 2, where the time series for pressure and the directional channels are shown for station 1. For Δp , a lead signal referenced to pressure represents North (for x-component) or East (for y-component), whereas a lag signal referenced to pressure represents South (for x-component) or West (for y-component). In Fig. 2 (a), Δp_x is lead, which represents North, whereas Δp_y is lag, representing West. Thus, it is clear that the source direction comes from the North-West quadrant. For p_v , if pressure and particle velocity are in-phase, it represents a signal from the North-East quadrant and vice-versa. In Fig. 2 (b), pressure and the estimated particle velocity p_{vx} are in-phase, whereas pressure and p_{vy} are in counter-phase. Thus, it represents a signal from the North-West quadrant as Δp .

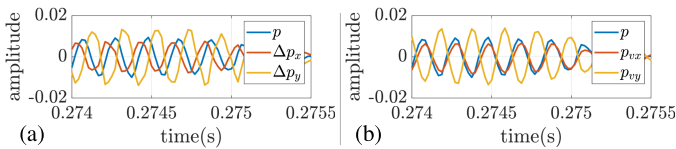


Fig. 2. Received time series at station 1: pressure and pressure-difference channels (a); and pressure and estimated particle velocity components (b).

The impact of the vector sensor channel combining on communications can be associated with the spatial filtering capability, analyzed here by the energy detection and azigrams. First, the beam response for station 1 is analyzed by varying the δ factor, where it is known that the source is at approximately -60° . In Fig. 3 (a), Δp is used, and the main lobe is noticed in the source direction, although ambiguity is verified as δ increases. In Fig. 3 (b), the ambiguity is mitigated and the maximum ratio between the main lobe and the sidelobe is found for $\delta = 0.5$. Figure 3 (c) shows the beam response with $\delta = 0.5$ for both Δp and p_v , where the ambiguity mitigation is apparent and the cardioid-like shaped response is obtained. Thus, one can conclude that the proper δ value is 0.5 for a backside ambiguity mitigation, which is set for quantifying the communication performance. Figure 3 (d) shows the azigrams for stations 1, 2, 5, and 6 (from top to bottom), where transmissions were performed at different geographic quadrants. Azigrams are analogous to spectrograms, but the color represents directions instead of power spectral density. Here, the azigrams also include transparency, where the intensity of each direction is taken into account (see details in [18] for displaying azigrams with transparency). The azigrams of Fig. 3 (d) were estimated using particle velocity channels as input in (9), $\Delta f = 100$ Hz with a frequency step of $f = 50$ Hz, and $\delta = 0.5$. The azigrams indicate four different source directions and how the dominant frequency band is related to each direction. Moreover, this figure indicates no ambiguity in frequency hopping modulation band, which is present in azigrams using pressure-difference channels (not shown due to lack of space).

B. Communication performance

The communication performance is quantified by two analyses: BER varying the azimuth angle of (7); and BER using

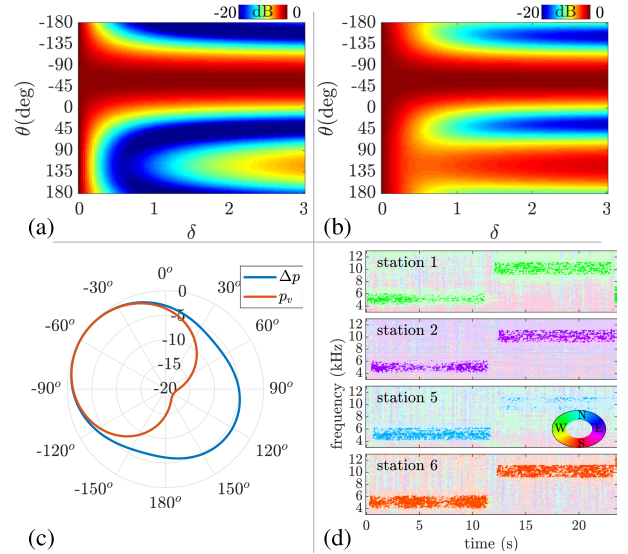


Fig. 3. Energy detection for varying δ for station 1 using Δp (a) and p_v (b). In (c), the beam response for Δp and p_v is compared for $\delta = 0.5$. Azigrams for stations 1, 2, 5, and 6 (d).

individual vector sensor channels or beam steering, for the six stations. Figure 4 shows the BER in a polar graphic from station 1 (a) to 6 (f) for the first analyzed band ($f_c = 5$ kHz). Note that the figure axis is inverted, where the error grows toward the center, which is normalized at 0.5. The BER is calculated by combining the vector sensor channels in the beam steering (y_{bs}), and it can be compared to the pressure channel (p). The figure is quite illustrative, combining directional information with BER performance. One can notice that a similar cardioid-like pattern is found but with some fluctuation. These are expected results since we are measuring the error that is also impacted by multipath. In general, for the beam steering, the minimum error is found in the source direction and is reduced by around 5% compared to the pressure channel.

Figure 5 shows the BER along the stations for the two analyzed frequency bands. The BER was quantified for the pressure-sensor, individual particle velocity channels, and beam steering using the DoA (bs). The beam steering approach resulted in a concise error reduction along the stations. Transmissions from stations two and three were predominantly towards the y-component, where the x-component SNR is decreased. Such geometry result in: the highest error for x-component due to low SNR; similar errors for y-component and beam steering. Among stations 3, 4, and 5, the transmissions were performed approximately at a radius of 2.2 km and varied the direction by 90° . As expected, the performance of the individual directional components changes, whereas the beam steering keeps the performance by combining the channels with the source direction. Another noticed aspect is

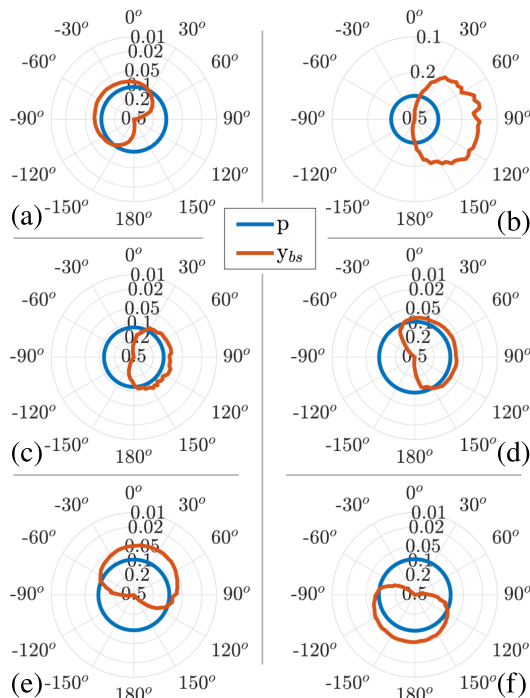


Fig. 4. Polar BER for stations 1 to 6, (a) to (f), respectively.

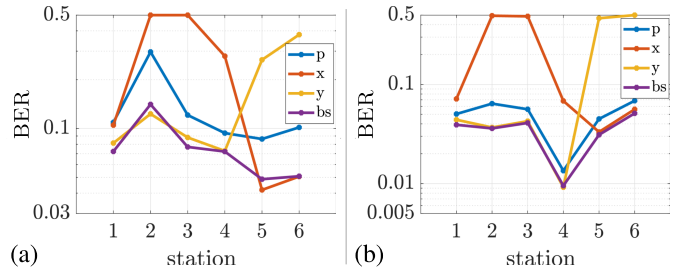


Fig. 5. BER along stations for pressure, individual particle velocity channels, and beam steering (bs), for $f_c = 5$ kHz (a) and $f_c = 10$ kHz (b).

that the outperformance of the beam steering is more effective in the lowest band. We have observed that above certain SNR, the performance of JANUS, before interleaved stage, cannot be enhanced by improving SNR, and ISI becomes the main issue. The SNR in the band of 10 kHz is higher than SNR at 5 kHz, which is related to source level (6 dB of difference between bands) and ambient noise. The SNR gain of the beam steering compared to pressure sensor is similar for both frequencies. However, since the overall SNR in the band of 5 kHz is lower, the impact of beam steering in the error is more perceptible. We expect that a similar enhancement would be found if the overall SNR for both frequency bands was similar.

V. CONCLUSION

The use of a single pressure-gradient vector sensor for underwater acoustic communications is experimentally investigated in this work. The vector sensor's directional characteristic was firstly compared between pressure-difference and particle velocity, where the latter may present a cardioid-like beam pattern. It was seen that a design factor can be set to achieve a desired beam pattern. Moreover, azigrams are an interesting way to see the frequency impact on the beam pattern. The BER performance was quantified for the frequency hopped JANUS modulation, where the direction information was related to the performance. A polar BER shows a similar cardioid-like pattern turned into the azimuth source direction, which demonstrates the theoretical impact. The BER for the transmitting stations at different geographic quadrants and at orthogonal directions shows that: the beam steering using estimated source direction outperforms the pressure sensor; the beam steering has similar or even better performance than individual directional channels; the ambiguity mitigation of the cardioid has a higher impact on the performance for the lowest band analyzed.

ACKNOWLEDGMENTS

This work was performed under the European Multidisciplinary Seafloor Observatory Portugal (EMSO-PT) project, and K2D - Knowledge and data from the deepspace (contract Ref. ISISE-125.21). The authors would like to thank the SiPLab participants in the EMSO'21. F. Bozzi thanks the support of the Brazilian Navy Postgraduate Study Abroad Program.

REFERENCES

- [1] C. H. Sherman and J. L. Butler, *Transducers and Arrays for Underwater Sound*. New York, NY: Springer New York, 2007.
- [2] T. Gabrielson, "Design problems and limitations in vector sensors," Naval Undersea Warfare Center Division and Office of Naval Research, Newport, Rhode Island, Proceedings of the Workshop on Directional Acoustic Sensors, Apr. 2001.
- [3] A. Abdi, H. Guo, and P. Suthiwan, "A new vector sensor receiver for underwater acoustic communication," in *OCEANS 2007*. Vancouver, BC: IEEE, Sep. 2007, pp. 1–10.
- [4] P. Felisberto, P. Santos, and S. M. Jesus, "Acoustic pressure and particle velocity for spatial filtering of bottom arrivals," *IEEE J. Oceanic Eng.*, vol. 44, no. 1, pp. 179–192, Jan. 2019.
- [5] G. D'Spain, J. Luby, G. Wilson, and R. Gramann, "Vector sensors and vector sensor line arrays: comments on optimal array gain and detection," *J. Acoust. Soc. Am.*, vol. 120, p. 171, Jul. 2006.
- [6] A. Nehorai and E. Paldi, "Acoustic vector-sensor array processing," *IEEE Trans. Signal Process.*, vol. 42, no. 9, pp. 2481–2491, Sept./1994.
- [7] K. B. Smith and A. V. van Leijen, "Steering vector sensor array elements with linear cardioids and nonlinear hippoids," *J. Acoust. Soc. Am.*, vol. 122, no. 1, pp. 370–377, Jul. 2007.
- [8] D. Levin, E. A. P. Habets, and S. Gannot, "Maximum likelihood estimation of direction of arrival using an acoustic vector-sensor," *J. Acoust. Soc. Am.*, vol. 131, no. 2, pp. 1240–1248, Feb. 2012.
- [9] H. Cao, W. Wang, L. Su, H. Ni, P. Gerstoft, Q. Ren, and L. Ma, "Deep transfer learning for underwater direction of arrival using one vector sensor," *J. Acoust. Soc. Am.*, vol. 149, no. 3, pp. 1699–1711, Mar. 2021.
- [10] A. Song, A. Abdi, M. Badiy, and P. Hursky, "Experimental demonstration of underwater acoustic communication by vector sensors," *IEEE J. Oceanic Eng.*, vol. 36, no. 3, pp. 454–461, Jul. 2011.
- [11] J. Potter, J. Alves, D. Green, G. Zappa, I. Nissen, and K. McCoy, "The janus underwater communications standard," in *2014 Underwater Communications and Networking (UComms)*. Sestri Levante, Italy: IEEE, Sep. 2014, pp. 1–4.
- [12] K. McCoy, V. Djapic, and M. Ouimet, "Janus: Lingua franca," in *OCEANS 2016 MTS/IEEE Monterey*. Monterey, CA, USA: IEEE, Sep. 2016, pp. 1–4.
- [13] "Anep-87 - digital underwater signalling standard for network node discovery and interoperability," NATO standardization office, Tech. Rep., Mar. 2017.
- [14] K. Pelekanakis, "Extending janus for faster bit rates," in *4th JANUS International Workshop*, La Spezia, Italy, 2019, Presentation.
- [15] F. A. Bozzi and S. M. Jesus, "Acoustic vector sensor underwater communications in the makai experiment," in *Proceedings of Meetings on Acoustics, 6th UACE*. Virtual Meeting: ASA, Jul. 2021, p. 070029.
- [16] —, "Joint vector sensor beam steering and passive time reversal for underwater acoustic communications," *IEEE Access*, vol. 10, pp. 66 952–66 960, Jun. 2022.
- [17] B. Armstrong, *M35-300 Directional Hydrophone*, 10 Akerley Boulevard, Unit 19, Dartmouth, Nova Scotia B3B 1J4, Apr. 2020.
- [18] A. M. Thode, T. Sakai, J. Michalec, S. Rankin, M. S. Soldevilla, B. Martin, and K. H. Kim, "Displaying bioacoustic directional information from sonobuoys using "azigrams"," *J. Acoust. Soc. Am.*, vol. 146, no. 1, pp. 95–102, Jul. 2019.